Challenges in the development of chronic pulmonary hypertension models in large animals

Abraham Rothman[1,2], Robert G. Wiencek[3], Stephanie Davidson[4], William N. Evans[1,2], Humberto Restrepo[1,2], Valeri Sarukhanov[1] and David Mann[5]

[1]Children's Heart Center Nevada, Las Vegas, NV, USA; [2]University of Nevada, School of Medicine, Department of Pediatrics, Las Vegas, NV, USA; [3]Stanford University, Department of Cardiothoracic Surgery, Cardiothoracic Dignity Healthcare, Las Vegas, NV, USA; [4]Anesthesiologist Consultants Inc., Las Vegas, NV, USA; [5]Vascular BioSciences, Goleta, CA, USA

Abstract

Pulmonary hypertension (PH) results in significant morbidity and mortality. Chronic PH animal models may advance the study of PH's mechanisms, evolution, and therapy. In this report, we describe the challenges and successes in developing three models of chronic PH in large animals: two models (one canine and one swine) utilized repeated infusions of ceramic microspheres into the pulmonary vascular bed, and the third model employed a surgical aorto-pulmonary shunt. In the canine model, seven dogs underwent microsphere infusions that resulted in progressive elevation of pulmonary arterial pressure over a few months. In this model, pulmonary endoarterial tissue was obtained for histology. In the aorto-pulmonary shunt swine model, 17 pigs developed systemic level pulmonary pressures after 2–3 months. In this model, pulmonary endoarterial tissue was sequentially obtained to assess for changes in gene and microRNA expression. In the swine microsphere infusion model, three pigs developed only a modest chronic increase in pulmonary arterial pressure, despite repeated infusions of microspheres (up to 40 in one animal). The main purpose of this model was for vasodilator testing, which was performed successfully immediately after acute microsphere infusions. Chronic PH in large animal models can be successfully created; however, a model's characteristics need to match the investigational goals.

Despite new therapies, pulmonary hypertension (PH) continues to be associated with high morbidity and mortality. The pathophysiology of PH remains poorly understood. PH is defined as a mean pulmonary artery pressure (PAp) >25 mmHg and an increased pulmonary vascular resistance (PVR) of $\geq$3 Wood units/m^2.[1] Further PH characteristics include pulmonary arterial medial hypertrophy, intimal lesions, and adventitial thickening. Previous investigations describe experimental models of PH in rats, mice, dogs, sheep, pigs, cows, and apes.[2–15] Small animal models allow for a larger number of subjects and easier experimental manipulation than large animal models; nevertheless, large animal models may better reflect human pathophysiology than small animal models. Common methods for experimentally creating PH have included hypoxia, monocrotaline, embolic occlusion, and creation of aorto-pulmonary shunts.[2–14,16] We chose to create large animal models of PH with the intent of testing an endoarterial biopsy catheter, to learn more about the molecular biology of the pulmonary vascular bed, and to perform acute vasodilator testing. We used large animals because it allowed for

Corresponding author:
Abraham Rothman, Children's Heart Center Nevada, 3006 S Maryland Parkway, Ste 690, Las Vegas, NV 89109, USA.
Email: arothman@childrensheartcenter.com

interventions such as cardiac catheterization and biopsy. The microsphere models appeared relatively simple to create and had some similarities to thromboembolic and pulmonary arterial obstructive diseases. The shunt model developed systemic level PH in one lung, allowed us to perform sequential biopsies, and had similarities to several congenital cardiac lesions. The purpose of this report is to describe to other investigators, clinicians, and trainees the challenges that we encountered in the sequential creation of three large animal models of PH with the purpose of helping them in selecting models, modifications, and techniques for their experimental endeavors.

Methods

The studies conformed to the Guide for the Care and Use of laboratory animals.[17] The University of California at San Diego Animal Subjects Committee approved the canine microsphere model. The University of Nevada Las Vegas Institutional Animal Subjects Committee approved the swine shunt and microsphere models.

Canine ceramic microsphere embolization model (canine bead model)

Ten mongrel dogs with a weight of 25.0 ± 5 kg and a mean age of 25.6 ± 15.6 months underwent an initial catheterization to obtain baseline hemodynamics and baseline biopsies. Animals were pre-anesthetized with 10 mg/kg of propofol, intubated, ventilated at a rate of 12–18 breaths/min, and given maintenance anesthesia with 1.5–2.0% isoflurane. An arterial femoral line was placed for monitoring. An 8-F sheath was placed in an external jugular vein. An 8-F thermodilution catheter (Baxter-Edwards, Irvine, CA, USA) was used to obtain cardiac and pulmonary pressures and cardiac output. Endoarterial biopsy samples were obtained from 2–3 mm peripheral arteries, as described previously.[18,19]

To develop the hypertensive model, ceramic microspheres (3M, St Paul, MN, USA), with a mean diameter of 0.6–0.9 mm (Fig. 1) were delivered approximately once a month through an 11-F sheath placed in an external jugular vein. Biopsies and angiography were performed immediately after the microsphere infusions. Four-view perfusion lung scans using ^{99m}Tc-labeled macroaggregated albumin were obtained before and after each microsphere infusion procedure.

After euthanasia with intravenous Pentothal sodium (120 mg/kg), the heart and lungs were examined. Cross-sections of arteries were obtained for histologic examination.

Swine aorto-pulmonary shunt model (shunt model)

A total of 30 Micro Yucatan female swine (Sinclair Research Center, Windham, ME, USA) were used for the creation of an aorto-pulmonary shunt model of chronic PH. Mean body weight was 22.4 ± 5.3 kg and mean age at surgery was 7.3 ± 2.7 months.

A cardiac catheterization with pulmonary angiography and biopsy were performed at baseline, as described above for the canine bead model. The swine were pre-anesthetized with a mixture of ketamine hydrochloride (Ben Venue Laboratories, Inc., Bedford, OH, USA) 22 mg/kg, acepromazine (Vedco, Inc., St Joseph, MO, USA) 0.2 mg/kg, and atropine (Baxter Healthcare Corp., Deerfield, IL, USA) 0.05 mg/kg, intramuscularly. Induction and general anesthesia was attained with inhaled isoflurane (Baxter Healthcare Co., Deer Field, IL, USA) 0.5–2.0%. Fentanyl 0.03–0.05 mg/kg was given during the thoracotomy. The animals were ventilated at a rate of 12–18 breaths/min. One gram of cefazolin (West-Ward Pharmaceutical Corp., Eatontown, NJ, USA) was administered intramuscularly before the procedure and 12 h later. To prevent ventricular arrhythmias, amiodarone (Bioniche Pharma., Lake Forest, IL, USA) was administered at a dose of 10–12 mg/kg intravenously prior to the catheterization.
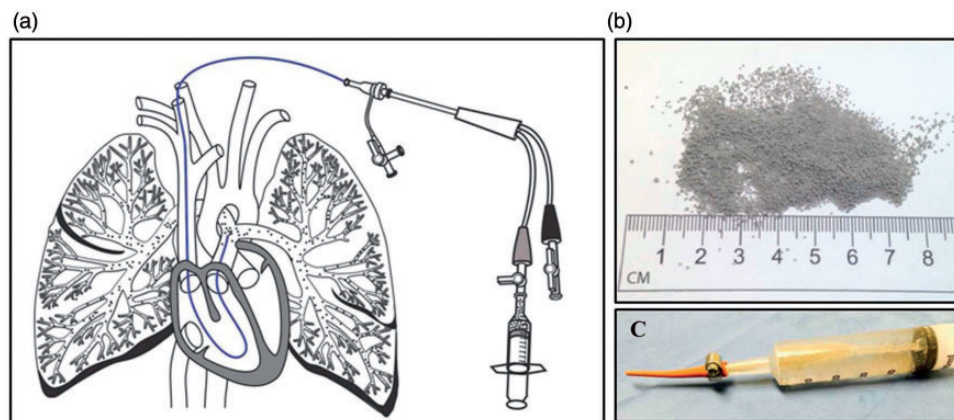
Fig. 1 Microspheres used for PH model creation: (a) Delivery configuration. The microspheres can be delivered through sheaths or catheters placed with the tip in the superior vena cava or the pulmonary arteries. (b) Ceramic microspheres. (c) Sixty milliliter syringe loaded with microspheres and adapted with a soft funneled tip that is placed into the proximal end of a 7–11-F long delivery sheath.

For surgical creation of the aorto-pulmonary shunt, a left thoracotomy was performed in the fourth intercostal space. The left pulmonary artery (LPA) was exposed, clamped, divided, and ligated at its origin from the pulmonary trunk. Heparin was given at a dose of 100 U/kg. The descending thoracic aorta was clamped and a window was created in its medial aspect by using a punch (ClearCut, Quest Medical Inc., Oconomowoc, WI, USA). An end-to-side anastomosis was created. After releasing the vascular clamp in the aorta, 2 mg/kg of furosemide (IVX Animal Health, Inc., St Joseph, MO, USA) was given. The chest was closed. No chest tube was placed in any of the animals.

Postoperatively, animals received furosemide orally (Vintage Pharmaceuticals, LLC, Huntsville, AL, USA), 2–4 mg/kg twice daily for 3–4 weeks, cephalexin (Teva Pharmaceuticals, North Wales, PA, USA) capsules, 500 mg twice a day for 10 days, and buprenorphine (Reckitt Benckiser Pharmaceutical, Parsippany, NJ, USA), 0.01–0.02 mg/kg twice daily for 3 days for pain and then as needed if the animals showed signs of pain. No chronic anti-coagulant or antiplatelet drugs were given until later in the study when intravascular thrombi became evident.

Catheterization with aortic pressure and LPA pressure measurement, angiography, and biopsies of the LPA were performed 1 week, 3 weeks, and monthly from 2 to 6 months after surgery. The hemodynamic assessment and biopsy methods were similar to those described above for the canine bead model, with the following exceptions: access was from a carotid artery, isolated by cutdown, and cannulated with an 8-F sheath. A cutoff 5-F pigtail catheter was used to enter the LPA from the proximal descending aorta using a Wholey wire. Pre- and post-biopsy angiograms in distal LPA branches were performed through the pigtail catheter or through the long sheath. The carotid artery was repaired using microsurgical technique.

Swine ceramic microsphere embolization model (swine bead model)

Nine Micro Yucatan female swine (Sinclair Research Center, Windham, ME, USA), with a mean weight of 24.9 ± 2.1 kg and a mean age of 6.2 ± 0.8 months, underwent a baseline cardiac catheterization with pulmonary angiography and biopsy, as described above for the canine bead model. Animals were pre-anesthetized, anesthetized, and given prophylactic amiodarone as described in the shunt model. The hemodynamic assessment, biopsy methods, and infusion of microspheres were similar to those described above for the canine bead model, with the following exceptions: access was via neck cutdown: an 8-F sheath was placed either in the internal or the external jugular vein and a 5-F sheath was placed in the common carotid artery to monitor arterial pressure. Microspheres were delivered approximately every 1–2 weeks through an 8-F sheath placed in a jugular vein. Microspheres were infused until the peak systolic pulmonary arterial systolic pressure was

5–10 mmHg higher than the maximum level obtained during the previous infusion procedure. Euthanasia and pathologic examination were performed as in the canine bead model.

Technical aspects

Access. Access in dogs was by percutaneous Seldinger technique, consisting of needle entry into the vessel, followed by a guide wire and then the sheath. Venous access was via an external jugular vein and arterial access via the femoral artery. In swine, venous and arterial access was by cutdown in the neck, the axillary area, or the femoral area.

Vessel re-entry. In order to perform sequential procedures, we discovered that we could obtain repeated access in veins and arteries, even if they were completely occluded by thrombus. Either by needle access or by performing a nick in the vessel with a blade, we could advance the guide wire into the vessel, followed by the sheath. At the end of each procedure, microsurgical techniques were used to repair the vessels, and in the last four animals we marked the vessels with vessel loops to permit easy identification and access at the next procedure.

Results

Canine bead model

The purpose of creating this model was to test an endoarterial biopsy catheter in pulmonary arteries with hypertension. Our original aim was to deliver enough beads to the pulmonary vascular bed to attain at least three-quarters of systemic level systolic PAp. Bead infusions resulted in acute pO_2 levels <50 mmHg. The first three dogs died or had to be euthanized shortly after a single infusion of beads. Therefore, the protocol was modified to give fewer beads at monthly intervals.

Two dogs were euthanized after two bead infusions. The average systolic PAp increased to 36 mmHg after the first infusion and to 45 mmHg after the second infusion. It became apparent that long-term survival was possible if bead infusions were stopped when the acute pO_2 levels reached about 60–70 mmHg. Subsequently, three dogs survived nine bead infusions and two dogs survived 12 infusions. One dog was kept alive for 32 months after the initial bead infusion, did well clinically, and by the time of euthanasia had a stable PAp at two-thirds of the systemic level.

Lung perfusion scans showed major areas of hypoperfusion distributed evenly in both lungs after each bead infusion, partial recovery of flow in between infusions, and larger and more persistent flow deficits after multiple bead infusions (Fig. 2).

Among the long-term survivors, the first three dogs received a total of 9 cc of beads each. The next two dogs received a total of 4 cc of beads initially and 3 cc at the
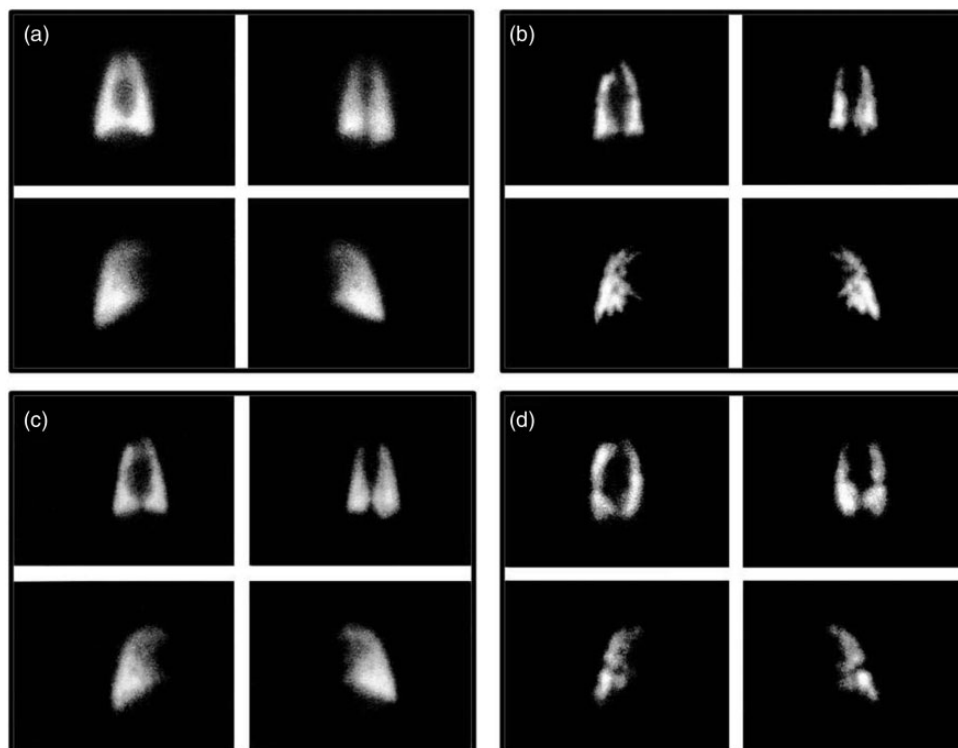
Fig. 2 Representative lung scans: antero-posterior (top left), postero-anterior (top right), right lateral (bottom left), and left lateral (bottom right) views. (a) Baseline. (b) Immediately after the first bead infusion. (c) Prior to the second bead infusion. (d) Prior to the last bead infusion.
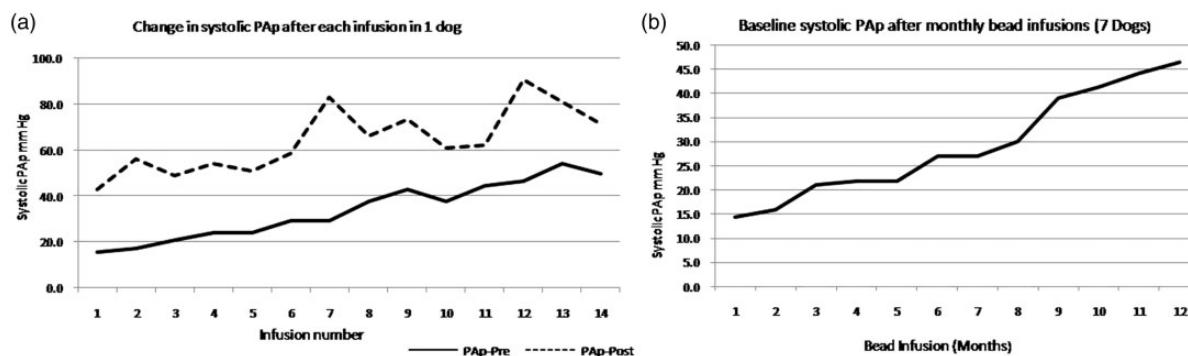
Fig. 3 Representative changes in systolic PAp after each microsphere infusion in one animal from the canine bead model (left). Average baseline systolic pressure in seven dogs after multiple microsphere infusions (right).

second infusion. Thereafter, infusions were given starting with approximately 0.2 cc of beads and slowly repeating the infusions every 15 min until the desired pO_2 was attained.

In the five dogs that survived multiple bead infusion procedures, the average mean PAp increased from 13 mmHg at baseline to 32 mmHg after the first infusion. A month later, the mean PAp decreased to 20 mmHg, increasing to 42 mmHg after the second infusion. This pattern of partial recovery of PAp between infusions was observed consistently. However, the immediate pre-bead infusion mean PAp increased progressively with increasing number of infusions (Fig. 3), reaching 40 mmHg after 9 months and 47 mmHg after 12 months. The highest systolic PAp attained acutely after a bead infusion was 100 mmHg.

In the long-term survivors, the average PVR increased from 2.4 Wood units at baseline to 7.7 Wood units after the first bead infusion. One month later, the PVR had decreased to 2.6 Wood units, increasing to 8.1 Wood units immediately after the second infusion. Again, a pattern of partial decrease in PVR between infusions occurred consistently, but the pre-bead infusion PVR increased progressively

with increasing number of infusion procedures, reaching an average of 6.5 Wood units at 9 months and 7.8 Wood units after 12 months. The highest acute PVR attained was 12.3 Wood units.

A total of 29 biopsy procedures were performed immediately after the bead infusions. Samples were retrieved with a success rate of 79%. There were no significant adverse clinical effects on the animals as a result of the biopsy procedures. Intimal flaps, vascular cuffing, and transient spasm were observed, but generally resolved on follow-up angiography.[18] The biopsy samples were adequate for histologic examination and demonstrated hypertensive changes, including thickened neointima, disorganized elastic laminae, and myxoid degeneration in the media.[18]

At necropsy, branches of the distal pulmonary vascular tree were variably filled with beads and intertwined with thrombus and neointima. Histologic examination of pulmonary arteries showed characteristic hypertensive changes.[18]
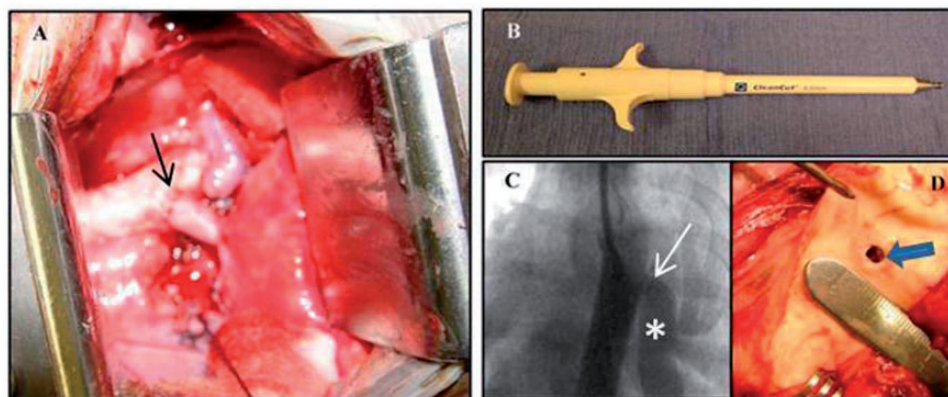
Shunt model

The purpose of this model was to create systemic level PH and do sequential biopsies to assess molecular changes with progression of the disease. Four micro-Yucatan swine underwent unrestricted anastomosis of the LPA to the descending aorta. All four animals died: three within a few hours and one 21 days after the surgery with signs of overwhelming pulmonary edema. At necropsy the size of the connection was estimated at 5–6 mm. The aortic window size for the anastomosis was then decreased to 4 mm. Two animals survived and developed systemic level PH in the left lung, at days 49 and 70 after surgery, respectively.

The protocol was then modified to include a baseline pulmonary arterial biopsy catheterization through the right heart prior to the surgery, thus procuring normal pressure endovascular tissue to compare with the hypertensive samples. However, two animals died with refractory ventricular fibrillation during guide wire (n = 1) and long sheath (n = 1)

passage through the right heart. Therefore, the technique was modified to use a softer guide wire and administering intravenous amiodarone prior to each procedure. The presurgical biopsy procedure was performed safely in all subsequent animals.

Use of a 4-mm window in the aorta resulted in failure to develop PH in two other animals and shunt obstruction/thrombosis in five animals, 39–91 days after surgery. To solve these difficulties, the window size in the aorta was increased to 4.5 mm (Fig. 4). A total of 17 swine survived the 6-month protocol and consistently developed near-systemic level PH in the left lung by 2–3 months (Fig. 5). LPA angiography performed after surgery but while the pressure was still normal, showed smooth and undistorted distal pulmonary artery branches. After the onset of severe PH, there was enlargement of proximal branches and tortuosity, narrowing, irregularities, and a reduction in number of distal LPA branches. Angiograms performed immediately after the biopsies generally showed patent and undistorted vessels, but occasionally there were partial stenoses or irregularities in the luminal contour, and very rarely complete occlusions, which generally resolved on follow-up angiography.[20] Cardiac catheterizations, including angiography and biopsies, were performed without significant complications, such as death, hypotension, arrhythmias, hemothorax, hemoptysis, or difficulties with weaning from anesthesia. Biopsy samples were adequate for histologic and molecular studies, including DNA microarray analysis,[21] and quantitation of microRNA expression at different stages of PAH.

At necropsy, the hypertensive left lung was grossly congested. The pulmonary arterial wall was thickened, with variable amounts of intraluminal thrombus, yellow discoloration, and irregular surfaces. Some vessels showed significant patchy sclerosis, which was impossible to cut with a sharp scalpel. Similar to the canine bead model, baseline pulmonary tissue showed normal histology, while hypertensive biopsy samples and necropsy specimens showed progressive thickening of the neo-intima, thickening and

Fig. 4 Images of shunt model creation. (a) Left pulmonary artery to aorta anastomosis (arrow) at the time of surgery. (b) Instrument used to perform a 4.5-mm punch. (c) Descending aortogram showing a patent anastomosis (arrow) and flow to the LPA (asterisk). (d) View of the hole punch, from the aortic side, at the time of necropsy.
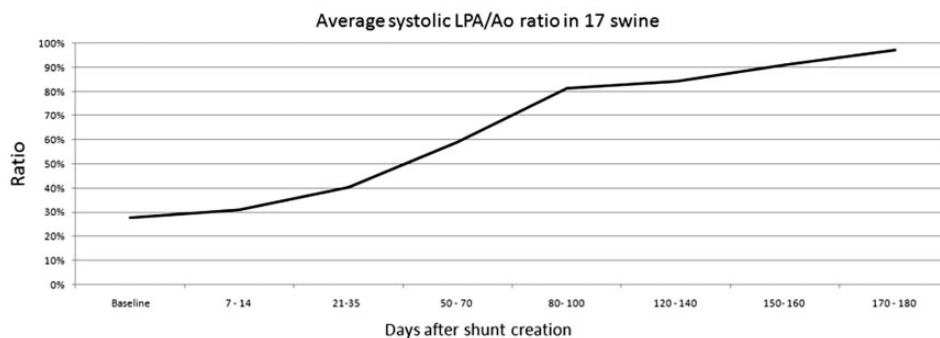
Fig. 5 LPA baseline systolic pressure (as a ratio of systemic systolic pressure) versus time after surgical shunt creation in 17 long-term surviving animals.
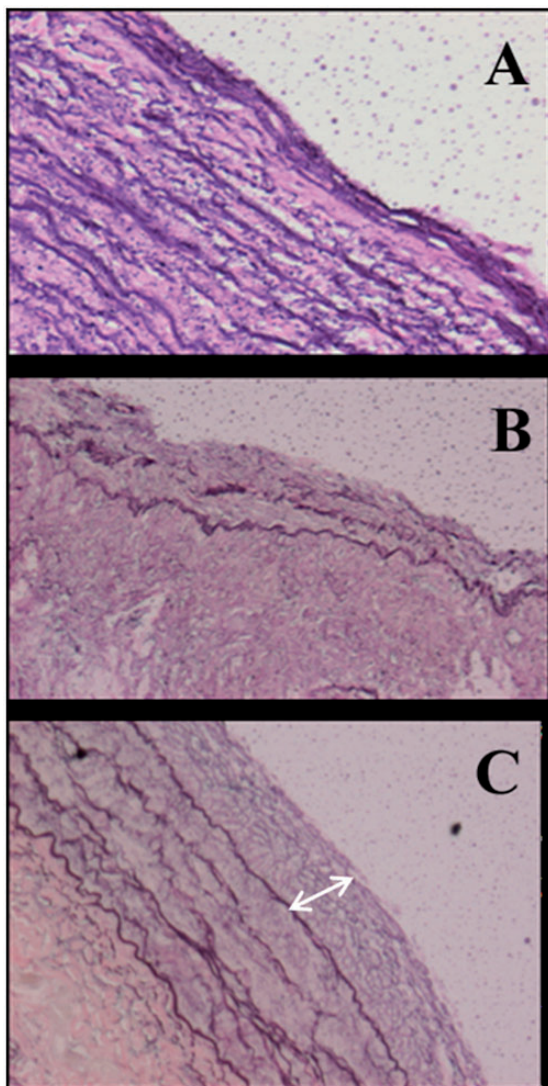

Fig. 6 Pulmonary artery endovascular histology using Elastin stain in the shunt model. (a) Normal right pulmonary artery. (b, c) Hypertensive left pulmonary artery: The elastic lamellae are disorganized and the neointima is significantly thickened (two-sided arrow).

degenerative changes in the media (Fig. 6), and plexiform-like lesions.[20]

Swine bead model

The purpose of this model was to create PH and perform acute vasodilator testing. Of the nine Micro-Yucatan swine subjected to repeated delivery of microspheres, two died after one bead infusion each, having attained acute systolic pulmonary arterial pressures of 55 and 45 mmHg, respectively. Two other animals died after two bead infusions each, having reached a systolic pulmonary arterial pressure of 40 and 58 mmHg at the second bead infusion, respectively. One animal died after three bead infusions, with a peak systolic pulmonary arterial pressure of 35, 43, and 45 at the three procedures, respectively. One animal had nine separate catheterizations and six bead infusions and ran out of arterial and venous access sites and was euthanized. We then modified the technique of leaving rubber vessel tie markers around the vein and artery at the end of each procedure (see ''Technical aspects'' below). Three animals survived in the long term after undergoing 21, 24, and 40 separate microsphere infusions, respectively. PAp increased acutely after each microsphere infusion and completely or partially recovered between infusions. The maximal baseline systolic PAp attained after the multiple microsphere infusions in the three animals was 35, 37, and 38 mmHg, respectively, despite attaining peak systolic pressures of 60–85 mmHg immediately after the bead infusions. Fig. 7 depicts representative changes in systolic PAp after each infusion in one animal and the mean increase in baseline systolic pressure in three animals after multiple microsphere infusions.

While the baseline PAp did not increase significantly after multiple microsphere infusions, it was possible to acutely increase the PAp to approximately three-quarters of the systemic level and perform acute vasodilator studies. We have been testing the effects of fasudil (a Rho Kinase inhibitor), treprostinil, and veletri, with and without the effects of a
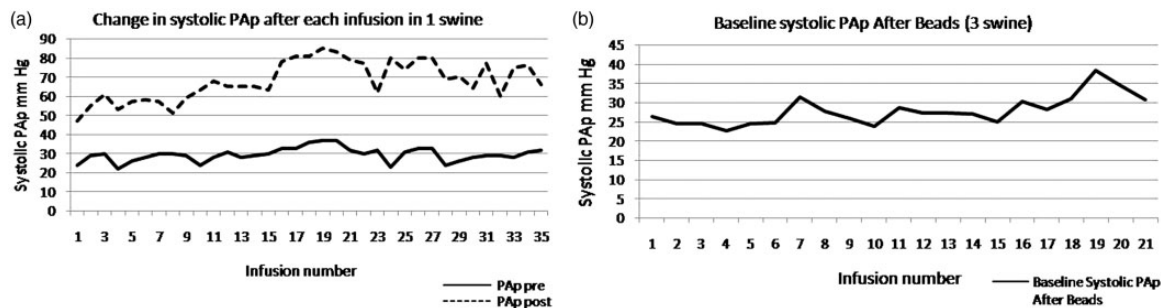
Fig. 7 Representative changes in systolic PAp after each microsphere infusion in one animal from the swine bead model (left). Average baseline systolic pressure in three animals after multiple microsphere infusions (right).
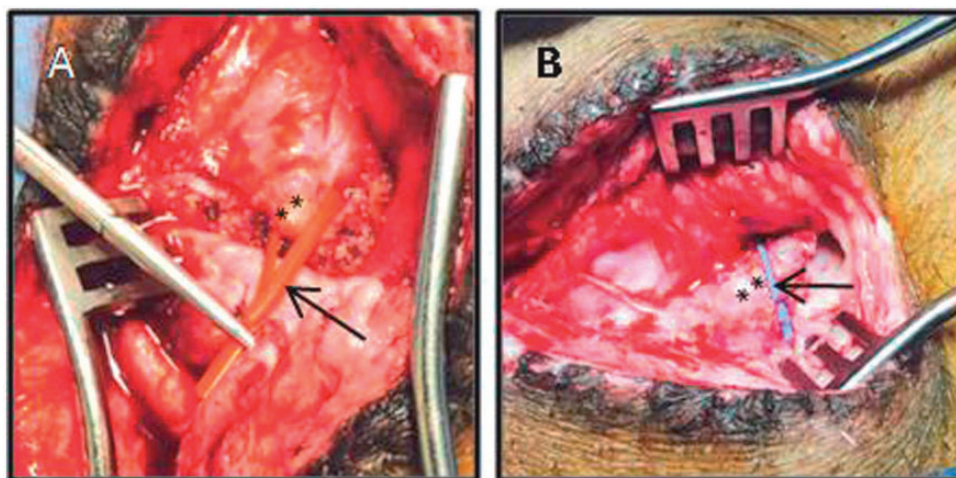
Fig. 8 Vessel rubber markers (arrows) placed at the end of the procedure around the (a) common carotid artery (asterisks) and (b) jugular vein (asterisks).

pulmonary vascular homing peptide CARSKNKDC (CAR) in acutely instrumented studies.[22,23]

Technical aspects

The relatively thin skin in dogs allowed for repeated percutaneous access to neck veins. However, the thicker skin in pigs required cutdowns for venous and arterial access. Marking the vein and artery just prior to wound closure facilitated finding the vessels at the subsequent procedure (Fig. 8). Re-canalization of completely thrombosed veins and arteries was generally possible and successful. Microsurgery was used to reconstruct the vessels at the end of each procedure. With these techniques, we were able to successfully perform more than 40 separate procedures in one animal via a neck cutdown.

Discussion

We present a chronologic account of our experience, including the technical details, creating chronic models of PH in large animals. The purpose of the canine bead model was to develop chronic PH in dogs and to test the safety and efficacy of a novel endoarterial biopsy catheter in obtaining sequential pulmonary arterial endovascular samples. The purpose of the aorto-pulmonary shunt model was to develop high-level PH in swine and assess whether the biopsy procedure could be performed safely and if the biopsy samples would be adequate for histologic and newer molecular studies. The purpose of the swine bead model was to attempt to recreate the canine bead model, with the aim of performing acute vasodilator studies.

The choice of dogs in the first model was based on previous experience with that species in the laboratory. Swine were chosen in the second model based on a published study.[24] The use of swine in cardiovascular research has been strongly supported by others.[25,26] Only female animals were used because of the higher propensity for development of PH in the experimental and the clinical setting and less aggressive behavior in the cages.[27–29] The third model was also created in swine based on the success in creating the swine shunt model and our previous success with the canine bead model. The canine and swine bead models have some similarities, at least mechanically, to clinical thromboembolic PH. The shunt model mimics systemic to pulmonary arterial shunts in humans including patent ductus arteriosus, Potts

shunts (anastomosis of the left pulmonary artery to the descending aorta), Waterston shunts (anastomosis of the right pulmonary artery to the ascending aorta), large Blalock-Taussig shunts, hemitruncus (origin of one of the pulmonary arteries from the ascending aorta), aorto-pulmonary windows, and perhaps even ventricular septal defects.

The advantages of the canine and swine bead models were the relative ease of delivery of beads through a jugular venous sheath at regular intervals, no need for a major surgical procedure, and creation of PH in both lungs. The canine bead model was successful for testing a novel endoarterial biopsy catheter in pulmonary arteries with pressures ranging from normal to systemic level PH. The limitation of this model was that with increasing numbers of microsphere infusions, the number of available vessels, which remained patent for biopsy, became more limited. The shunt model was created to allow sequential biopsies and analysis of genetic (mRNA and miRNA) changes as PH developed. In this model, single-sided systemic level PH was reached very reproducibly. However, the disadvantage of this model was that a few weeks after systemic level PH was attained, the vessels in that lung developed thrombi, even despite the implementation of daily anticoagulation with warfarin. In addition, we performed a preliminary study of vasodilator testing in the shunt model when the pressures were at systemic level. However, it was difficult to separate the decrease in left pulmonary arterial pressure from the decrease in aortic pressure (as the left pulmonary artery is connected directly to the descending aorta). We surgically implanted a flow probe in the proximal left pulmonary artery to assess the acute changes in pulmonary vascular resistance; however, scar developed between the pulmonary artery and the probe and limited its usefulness.

Both the canine and swine bead models offer an opportunity to study the mechanisms by which pressure and vascular resistance decrease in between bead infusions. Whether this occurs through dilation of pre-existing vessels, recruitment of superfluous vessels, or angiogenesis/vasculogenesis remains to be determined. In the swine bead model, we attempted to recreate the canine bead model. However, even after multiple separate microsphere infusions in the swine (40 in one animal), the baseline PH was only modestly elevated. The nature and mechanism of this potentially protective mechanism in swine during attempts to create systemic level PH by delivery of ceramic microspheres to the pulmonary vasculature awaits further study.

In the shunt model, the use of a 4.5-mm aortic window in the Micro Yucatan swine established a reproducible hemodynamic course, which resulted in two or three catheterizations in which LPA pressure was still normal, and several subsequent catheterizations and biopsy procedures in which severe PH had developed. This PH model could be used to test therapeutic agents or maneuvers at several hemodynamic and disease stages, including baseline, during a high flow but low LPA pressure state, and at the time of development of PH.

Several procedural details were important in the final development of the shunt model, starting with the size of the animals (20–22 kg) and the size of the aortic window at the time of surgery. Furosemide was continued twice a day for 3–4 weeks. No chest tube was necessary after the surgeries. Antibiotics were continued for 10 days after surgery and reinstituted when animals had increased cough or fevers. Intravenous amiodarone may have prevented arrhythmias during intracardiac wire and catheter manipulations. Initially in the study, neither antiplatelet agents nor anticoagulants were used, except for heparin during the surgery and catheterization procedures. However, two animals showed significant thrombi in the LPA vascular tree at necropsy, one with complete occlusion by thrombus from the aorto-LPA anastomosis to the periphery. Therefore, in the last five animals, we used daily warfarin and were still unable to completely prevent clotting. We would still recommend a trial of antiplatelet or anticoagulant agents, at perhaps higher doses, if animals are maintained experimentally longer than a few weeks after developing PH. An additional procedural improvement was the marking of the vein and artery with a vessel loop at the end of the procedure. This allowed faster dissection, less trauma, and decreased subsequent scarring around the vessels and the access site.

In these studies, we used an endoarterial biopsy catheter, which allowed pulmonary endoarterial biopsy procedures to be performed sequentially as the PH models developed. The catheter was safe and effective. Biopsy samples were adequate for cell culture and propagation of smooth muscle and endothelial cells,[19] histology and the study of mRNA[21] and microRNA changes. We have also shown previously that biopsy samples obtained in an experimental model of lung transplantation were adequate for polymerase chain reaction (PCR) analysis and that molecular changes in VCAM-1 mRNA levels were observed earlier than histologic changes of lung transplant rejection.[30]

Prostacyclin analogs, endothelin blockers phosphodiesterase 5 inhibitors, and guanylate cyclase stimulators have been approved for treatment of patients with PH.[31–39] However, PH continues to be a severe disease with significant morbidity and mortality. To better understand the mechanisms leading to PH and to develop improved therapies, it would be helpful to study animal models and device techniques to obtain pulmonary vascular tissue in animals and humans. PH has been created in small animal models, including mice and rats, with hypoxia,[2–5] monocrotaline,[6–14] genetic modifications,[9,40–42] and surgical shunts[16] One of the limitations of these models is the difficulty with chronic hemodynamic and tissue monitoring. Larger animal models, including, pigs, sheep, dogs, macaques, calves, and apes, have also been created with hypoxia,[43–50] monocrotaline,[51–53] infectious agents,[15] air infusions,[54] carotid to jugular vein anastomoses,[55] ligation of pulmonary veins,[56] systemic to pulmonary arterial shunts, surgical pulmonary artery ligation, and microsphere infusions.[18,19,22,57–63] They have added significantly to the understanding of PH.

There are several limitations to our models. As always, animals may not exactly reflect the changes or the rate of development of PH that occur in humans. For the bead models, the beads mechanically obstruct pulmonary arteries but may lack many of the mediators present in chronic emboli that affect the pulmonary vasculature. For the shunt model, no direct assessment of LPA vascular resistance was performed because the amount of flow through the left lung was difficult to quantitate.

Animal models will continue to be essential to further our understanding of and develop improved therapies for PH. In this paper, we summarized our experience, including the difficulties and successes, in creating three long-term models of PH in large animals. The choice of species and method of PH creation should depend on the aims of each investigation. The advantages and drawbacks of each model need to be recognized. We describe a significant difference in the chronic response of the pulmonary vasculature to repeated infusion of microspheres in dogs compared to pigs. Elucidating the nature of the resistance or compensatory response to the development of chronic high levels of PH in pigs may offer clues that could be useful in designing new therapies for patients with PH.

References

1. Rosenzweig EB, Widlitz AC and Barst RJ. Pulmonary arterial hypertension in children. *Pediatr Pulmonol* 2004; 38: 2–22.
2. Laudi S, Steudel W, Jonscher K, et al. Comparison of lung proteome profiles in two rodent models of pulmonary arterial hypertension. *Proteomics* 2007; 7: 2469–2478.
3. Stenmark KR, Fagan KA and Frid MG. Hypoxia-induced pulmonary vascular remodeling: cellular and molecular mechanisms. *Circ Res* 2006; 99: 675–691.
4. Chen SJ, Chen IF, Meng QC, et al. Endothelin-receptor antagonist bosentan prevents and reverses hypoxic pulmonary hypertension in rats. *J Appl Physiol* 1995; 79: 2122–2131.
5. Drexler ES, Bischoff JE, Slifka AJ, et al. Stiffening of the extrapulmonary arteries from rats in chronic hypoxic pulmonary hypertension. *J Res Nat Instit Stand Technol* 2008; 113: 239–249.
6. Kolettis T, Vlahos AP, Louka M, et al. Characterization of a rat model of pulmonary arterial hypertension. *Hellenic J Cardiol* 2007; 48: 206–210.
7. Clozel M, Hess P, Rey M, et al. Bosentan, Sildenafil, and their combination in the monocrotaline model of pulmonary hypertension in rats. *Exp Biol Med* 2006; 231: 967–973.
8. Schermuly RT, Kreisselmeier KP, Ghofrani HA, et al. Chronic sildenafil treatment inhibits monocrotaline-induced pulmonary hypertension in rats. *Am J Resp Crit Care Med* 2004; 169: 39–45.
9. Ivy DD, McMurtry IF, Colvin K, et al. Development of occlusive neointimal lesions in distal pulmonary arteries of endothelin B receptor-deficient rats: a new model of severe pulmonary arterial hypertension. *Circulation* 2005; 111: 2988–2996.
10. Nishimura T, Faul JL, Berry GJ, et al. Effect of aortocaval fistula on monocrotaline-induced pulmonary hypertension. *Crit Care Med* 2003; 31: 1213–1218.
11. Mathew R, Zeballos GA, Tun H, et al. Role of nitric oxide and endothelin-1 in monocrotaline-induced pulmonary hypertension. *Cardiovasc Res* 1995; 30: 739–746.
12. Frasch HF, Marshall C and Marshall BE. Endothelin-1 is elevated in monocrotaline pulmonary hypertension. *Am J Physiol* 1999; 276: L304–L310.
13. Guignabert C, Raffestin B, Raoul W, et al. Serotonin transporter inhibition prevents and reverses monocrotaline pulmonary hypertension in rats. *Circulation* 2005; 111: 2812–2819.
14. White RJ, Meoli DF, Swarthout RF, et al. Plexiforme-like lesions and increased tissue factor expression in a rat model of severe pulmonary hypertension. *Am J Physiol Lung Cell Mol Physiol* 2007; 293: L583–L590.
15. Marecki JC, Cool CD, Parr JE, et al. HIV-1 Nef is associated with complex pulmonary vascular lesions in SHIV-nef–infected macaques. *Am J Respir Crit Care Med* 2006; 174: 437–445.
16. Jungebluth P, Ostertag H and Macchiarini P. An experimental animal model of postobstructive pulmonary hypertension. *J Surg Res* 2008; 147: 75–78.
17. Committee for the update of the guide for the care and use of laboratory animals. *Guide for the care and use of laboratory animals*. 8th ed. Washington, DC: National Academy Press, 2011.
18. Rothman A, Mann DM, Behling CA, et al. Percutaneous pulmonary endoarterial biopsy in an experimental model of pulmonary hypertension. *Chest* 1998; 114: 241–250.
19. Rothman A, Mann DM, House MT, et al. Transvenous procurement of pulmonary artery smooth muscle and endothelial cells using a novel endoarterial biopsy catheter in a canine model. *J Am Coll Cardiol* 1996; 27: 218–224.
20. Rothman A, Wiencek RG, Davidson S, et al. Hemodynamic and histologic characterization of a swine (Sus scrofa domestica) model of chronic pulmonary hypertension. *Comp Med* 2011; 61: 258–262.
21. Rothman A, Davidson S, Wiencek RG, et al. Vascular histomolecular analysis by sequential endoarterial biopsy in a shunt model of pulmonary hypertension. *Pulm Circ* 2013; 3: 50–57.
22. Mann D, Rothman A, Restrepo H, et al. CARSKNKDC (CAR) Selective enhancement of Fasudil-induced pulmonary vasodilation in a porcine model of chronic pulmonary hypertension. Poster session presented at: American Thoracic Society 2016 International Conference; 2016 May 16; San Francisco, CA.
23. Toba M, Alzoubi A, O'Neill K, et al. A novel vascular homing peptide strategy to selectively enhance pulmonary drug

efficacy in pulmonary arterial hypertension. *Am J Pathol* 2014; 184: 369–375.

24. Corno AF, Tozzi P, Genton CY, et al. Surgically induced unilateral pulmonary hypertension: time-related analysis of a new experimental model. *Eur J Cardio-Thoracic Surg* 2003; 23: 513–517.

25. Lelovas PP, Kostomitsopoulos NG and Xanthos TT. A comparative anatomic and physiologic overview of the porcine heart. *J Am Assoc Lab Anim Science* 2014; 53: 432–438.

26. Kuzmuk KN and Schook LB. Pigs as a model for biomedical sciences. In: Rothschild MF and Ruvinsky A (eds) *The Genetics of the Pig*, 2nd ed. Wallingford: CAB International, 2011, pp.426–444.

27. Dempsie Y, Nilsen M, White K, et al. Development of pulmonary arterial hypertension in mice over-expressing S100A4/Mts1 is specific to females. *Respir Res* 2011; 12: 159.

28. Austin ED, Lahm T, West J, et al. Gender, sex hormones, and pulmonary hypertension. *Pulm Circ* 2013; 3: 294–314.

29. Dempsie Y and MacLean MR. The influence of gender on the development of pulmonary arterial hypertension. *Exp Physiol* 2013; 98: 1257–1261.

30. Rothman A, Mann D, Behling CA, et al. Increased expression of endoarterial vascular cell adhesion molecule-1 mRNA in an experimental model of lung transplant rejection: diagnosis by pulmonary arterial biopsy. *Transplantation* 2003; 75: 960–965.

31. Rosenzweig EB and Barst RJ. Pulmonary arterial hypertension in children: A medical update. *Indian J Pediatr* 2009; 76: 77–81.

32. Barst RJ, Simonneau G, Rich S, et al. Efficacy and safety of chronic subcutaneous infusion of UT-15 (Uniprost) in pulmonary arterial hypertension (PAH). *Circulation* 2000; 102: li.100–li.101.

33. Olschewski H, Simonneau G, Galie N, et al. Aerosolized Iloprost Randomized Study Group. Inhaled iloprost for severe pulmonary hypertension. *N Engl J Med* 2002; 347: 322–329.

34. Hallioglu O, Dilber E and Celiker A. Comparison of acute hemodynamic effects of aerosolized and intravenous iloprost in secondary pulmonary hypertension in children with congenital heart disease. *Am J Cardiol* 2003; 92: 1007–1009.

35. Rosenzweig EB, Ivy DD, Widlitz A, et al. Effects of long-term bosentan in children with pulmonary arterial hypertension. *JACC* 2005; 46: 697–704.

36. Maiya S, Hislop AA, Flynn Y, et al. Response to bosentan in children with pulmonary hypertension. *Heart* 2006; 92: 664–670.

37. van Loon RL, Hoendermis ES, Duffels MG, et al. Long-term effect of bosentan in adults versus children with pulmonary arterial hypertension associated with systemic-to pulmonary shunt: does the beneficial effect persist? *Am Heart J* 2007; 154: 776–782.

38. Galie N, Badesch D, Oudiz R, et al. Ambrisentan therapy for pulmonary arterial hypertension. *JACC* 2005; 46: 529–535.

39. Galie N, Ghofrani H, Torbicki A, et al. Sildenafil citrate therapy for pulmonary arterial hypertension. *N Engl J Med* 2005; 353: 2148–2157.

40. Beppu H, Ichinose F, Kawai N, et al. BMPR-II heterozygous mice have mild pulmonary hypertension and an impaired pulmonary vascular remodeling response to prolonged hypoxia. *Am J Physiol Lung Cell Mol Physiol* 2004; 287: L1241–L1247.

41. Song Y, Jones JE, Beppu H, et al. Increased susceptibility to pulmonary hypertension in heterozygous BMPR2-mutant mice. *Circulation* 2005; 112: 553–562.

42. West J, Fagan K, Steudel W, et al. Pulmonary hypertension in transgenic mice expressing a dominant-negative BMPRIIgene in smooth muscle. *Circ Res* 2004; 94: 1109–1114.

43. Das M, Dempsey EC, Reeves JT, et al. Selective expansion of fibroblast subpopulations from pulmonary artery adventitia in response to hypoxia. *Am J Physiol Lung Cell Moll Physiol* 2002; 282: L976–L986.

44. Stenmark KR, Fasules J, Hyde DM, et al. Severe pulmonary hypertension and arterial adventitia changes in newborn calves at 4300 m. *J Appl Physiol* 1987; 62: 821–830.

45. Berkenbosch JW, Baribeau J and Perreault T. Decreased synthesis and vasodilation to nitric oxide in piglets with hypoxia-induced pulmonary hypertension. *Am J Physiol Lung Cell Mol Physiol* 2000; 278: L276–L283.

46. Sugiura T, Suzuki S, Hussein MH, et al. Usefulness of a new Doppler index for assessing both ventricular functions and pulmonary circulation in newborn piglets with hypoxic pulmonary hypertension. *Pediatr Res* 2003; 53: 927–932.

47. Sato H, Hall CM, Griffith GW, et al. Large animal model of chronic pulmonary hypertension. *ASAIO J* 2008; 54: 396–400.

48. Shelub I, van Grondelle A, McCullogh R, et al. A model of embolic chronic pulmonary hypertension in the dog. *J Appl Physiol* 1984; 56: 810–815.

49. Kim H, Yung GL, Marsh JJ, et al. Endothelin mediates pulmonary vascular remodeling in a canine model of chronic pulmonary hypertension. *Eur Respir J* 2000; 15: 640–648.

50. Perkett EA, Davidson JM and Meyrick B. Sequence of structural change and elastin peptide release during vascular remodeling in sheep with chronic pulmonary hypertension induced by air embolization. *Am J Pathol* 1991; 139: 1319–1332.

51. Gust R and Schuster DP. Vascular remodeling in experimentally induced subacute canine pulmonary hypertension. *Exp Lung Res* 2001; 27: 1–12.

52. Okada M, Yamashita C, Okada M, et al. Establishment of canine pulmonary hypertension with dehydromonocroltaline: importance of a larger animal model for lung transplantation. *Transplantation* 1995; 60: 9–13.

53. Chen EP, Bittner HB, Davis RD, et al. Right ventricular failure - Insights provided by a new model of chronic pulmonary hypertension. *Transplantation* 1997; 63: 209–216.

54. Zhou X, Wang D, Castro CY, et al. A pulmonary hypertension model induced by continuous pulmonary air embolization. *J Surg Res* 2011; 170: e11–e16.

55. Wu J, Luo X, Huang Y, et al. Hemodynamics and right ventricle functional characteristics of a swine carotid artery-jugular vein shunt model of pulmonary arterial hypertension: an 18-month experimental study. *Exp Biol Med* 2015; 240: 1362–1372.

56. Guihaire J, Haddad F, Noly PE, et al. Right ventricular reserve in a piglet model of chronic pulmonary hypertension. *Eur Respir J* 2015; 45: 709–717.

57. Muller WH, Dammann JF and Head WH. Changes in the pulmonary vessels produced by experimental pulmonary hypertension. *Surgery* 1953; 34: 363–375.

58. Rendas A and Reid L. Aorta-pulmonary shunts in growing pigs. Functional and structural assessment of the changes in the pulmonary circulation. *J Thorac Cardiovasc Surg* 1979; 77: 109–118.

59. De Canniere D, Stefanidis C, Brimioulle S, et al. Effects of a chronic aorto-pulmonary shunt on pulmonary hemodynamics in pigs. *J Appl Physiol* 1994; 77: 1591–1596.
60. Rondelet B, Kerbaul F, Motte S, et al. Bosentan for the prevention of overcirculation-induced experimental pulmonary arterial hypertension. *Circulation* 2003; 107: 1329–1335.
61. Rosenkrantz JG, Carlisle JH, Lynch FP, et al. Ligation of a single pulmonary artery in the pig: a model of chronic pulmonary hypertension. *J Surg Res* 1973; 15: 67–73.
62. Ferguson DJ, Berkas EM and Varco RL. Circulatory factors contributing to alterations in pulmonary vascular histology. *Surg Forum* 1953; 4: 267–270.
63. Mercier O, Tivane A, Raoux F, et al. A reliable piglet model of chronic thrombo-embolic pulmonary hypertension. *Am J Resp Crit Care Med* 2011; 183: A2415.